

Kinematic Parameters of Young Subsystems and the Galactic Rotation Curve

M. V. Zabolotskikh^{1*}, A. S. Rastorguev^{1,2}, and A. K. Dambis²

¹*Moscow State University, Vorob'evy gory, Moscow, Russia*

²*Sternberg Astronomical Institute, Universitetskii pr. 13, Moscow, 119992 Russia*

Received February 1, 2002

Abstract—We analyze the space velocities of blue supergiants, long-period Cepheids, and young open star clusters (OSCs), as well as the H I and H II radial-velocity fields by the maximum-likelihood method. The distance scales of the objects are matched both by comparing the first derivatives of the angular velocity Ω' determined separately from radial velocities and proper motions and by the statistical-parallax method. The former method yields a short distance scale (for $R_0 = 7.5$ kpc, the assumed distances should be increased by 4%), whereas the latter method yields a long distance scale (for $R_0 = 8.5$ kpc, the assumed distances should be increased by 16%). We cannot choose between these two methods. Similarly, the distance scale of blue supergiants should be shortened by 9% and lengthened by 3%, respectively. The H II distance scale is matched with the distance scale of Cepheids and OSCs by comparing the derivatives Ω' determined for H II from radial velocities and for Cepheids and OSCs from space velocities. As a result, the distances to H II regions should be increased by 5% in the short distance scale. We constructed the Galactic rotation curve in the Galactocentric distance range 2–14 kpc from the radial velocities of all objects with allowance for the difference between the residual-velocity distributions. The axial ratio of the Cepheid+OSC velocity ellipsoid is well described by the Lindblad relation, while $\sigma_u \approx \sigma_v$ for gas. The following rotation-curve parameters were obtained: $\Omega_0 = (27.5 \pm 1.4)$ km s⁻¹ kpc⁻¹ and $A = (17.1 \pm 0.5)$ km s⁻¹ kpc⁻¹ for the short distance scale ($R_0 = 7.5$ kpc); and $\Omega_0 = (26.6 \pm 1.4)$ km s⁻¹ kpc⁻¹ and $A = (15.4 \pm 0.5)$ km s⁻¹ kpc⁻¹ for the long distance scale ($R_0 = 8.5$ kpc). We propose a new method for determining the angular velocity Ω_0 from stellar radial velocities alone by using the Lindblad relation. Good agreement between the inferred Ω_0 and our calculations based on space velocities suggests that the Lindblad relation holds throughout the entire sample volume. Our analysis of the heliocentric velocities for samples of young objects reveals noticeable streaming motions (with a velocity lag of ~ 7 km s⁻¹ relative to the LSR), whereas a direct computation of the perturbation amplitudes in terms of the linear density-wave theory yields a small amplitude for the tangential perturbations. © 2002 MAIK “Nauka/Interperiodica”.

Key words: *Galactic kinematics, rotation curve, distance scale*

INTRODUCTION

The study of the kinematics of Galactic subsystems remains one of the most important fields of Galactic astronomy. The parameters of the Galactic rotation curve were determined repeatedly from HI and HII data (Clemens 1985; Fich *et al.* 1989; Merrifield 1992; Brandt and Blitz 1993; Nikiforov and Petrovskaya 1994; Honma and Sofue 1997; Nikiforov 1999) and stellar radial velocities (Karimova and Pavlovskaya 1973; Pont *et al.* 1994; Dambis *et al.* 1995; Glushkova *et al.* 1998). High-precision proper motions and trigonometric parallaxes that became available with the release of the HIPPARCOS catalog (The HIPPARCOS and TYCHO catalogs, ESA SP-1200, 1997) stimulated further works aimed at

refining the angular velocity Ω_0 and the form of the rotation curve in the local solar neighborhood (Feast *et al.* 1998; Rastorguev *et al.* 1999; Dambis *et al.* 2001). It should be pointed out that the reliability of the resulting rotation curves depends first and foremost on the correctness of the adopted distance scale of objects under study. Objects with known distances—classical Cepheids, open star clusters (OSC), and OB-associations—allow the rotation curve to be determined only out to heliocentric distances of 4–5 kpc, whereas H I and H II kinematic data allow constructing the rotation curve over a considerably wider interval of Galactocentric distances. The main problem is that the distances of giant molecular clouds (GMC) and, consequently, those of H II-regions, are determined from their single hot exciting stars whose distance scale is prone not

*E-mail: zabolot@lnfm1.sai.msu.ru

only to random but also to systematic errors. In this paper we matched for the first time the distance scale of GMC to the most accurately determined (in the random and systematic sense) distances, i.e., those of long-period classical Cepheids and OSC, and inferred the kinematic parameters using an algorithm that allows for initial-data errors, for the ellipsoidal distribution of residual velocities, and for the errors of systemic radial velocities that result from the propagation of distance errors (Rastorguev 2001).

Our second task was to compute the parameters of the spiral pattern of the Galaxy. Selection effects, i.e., the incompleteness of the sample due to interstellar extinction, makes it very difficult to localize spiral waves by analyzing only the space distribution of young objects. The use of kinematic data appears to be a more promising approach, because it is insensitive to selection effects (Mishurov *et al.* 1979). Thus Mishurov *et al.* (1997) determined, by analyzing the radial velocities of classical Cepheids exclusively, the principal parameters of the spiral pattern including the velocity-field perturbation amplitudes and concluded that the Sun is located near the corotation circle. The perturbations due to the spiral density wave are comparable in magnitude to the velocity dispersion of young subsystems. Therefore, only after the release of the HIPPARCOS and TYCHO-2 catalogs making high-precision proper motions available did it become possible to analyze the space velocity field of young objects. Torra *et al.* (2000) used the radial velocities of OB-stars and Cepheids and HIPPARCOS proper motions of these objects to infer a pattern speed of $\Omega_P \approx (31 \pm 4) \text{ km s}^{-1} \text{ kpc}^{-1}$. Lepine *et al.* (2001) also concluded that the Sun is near the corotation circle by assuming a superposition of a two- and four-armed pattern. At the same time, Rastorguev *et al.* (2001) concluded that the Sun is inside the corotation circle by analyzing long-period Cepheids and young OSC, and Mel'nik *et al.* (2001) came to the same conclusion based on their study of the pattern of systematic noncircular motions of OB-associations. Here we explore this issue further.

OBSERVATIONAL DATA

We used young OSC and long-period Cepheids as a reference sample for matching the distance scales of various objects. Our reference sample included 89 young OSC with $\log T < 7.6$ and heliocentric distances determined by Dambis (1999) by fitting Kholopov's (1980) ZAMS with an allowance for evolutionary deviations based on Geneva-group isochrones (Maeder and Meynet 1991). The radial velocities of cluster members were determined by Glushkova based on published data and can be found in the paper by Rastorguev *et al.* (1999). The proper

motions of clusters were computed from those of their member stars found in the HIPPARCOS catalog (Baumgardt *et al.* 2000).

Our reference sample included 113 classical Cepheids with periods $P > 9^d$ (or ages $\log T < 7.6$ as implied by the period-age relation of Efremov (1989)) and heliocentric distances computed using the fundamental-mode period-luminosity relation of Berdnikov *et al.* (1996):

$$\langle M_K \rangle_I = -5.46^m - 3.52^m \log P$$

in accordance with the procedure described therein. An earlier statistical-parallax analysis (Rastorguev *et al.* 1999) showed that the sample of Cepheids with shorter periods is not homogeneous in terms of pulsation mode and may be contaminated by first-overtone pulsators. We used published Cepheid radial velocities and HIPPARCOS proper motions. Young OSC and long-period Cepheids make up a kinematically homogeneous sample consisting of 176 and 142 objects with radial velocities and proper motions, respectively, including 124 objects with space velocities.

We performed a separate analysis of a blue-supergiant sample consisting of 102 stars with heliocentric distances tied to the OSC distance scale (Dambis 1990). The kinematic data for these stars were compiled by A.K. Dambis with the proper motions adopted from the HIPPARCOS catalog, and radial velocities, from the catalogs of Barbier-Brossat and Figon (2000) and Wilson-Evans-Batten (WEB) (Duflot *et al.* 1995).

Brandt and Blitz (1993) published the distances and radial velocities for a total of 206 H II-regions. We selected 203 of these objects with spectroscopic or photometric distances inferred from their exciting stars. The radial velocities of H II-regions were determined from the CO (2.2.-mm) radio lines of their associated molecular clouds. We did not include three H II-regions in the final list because of their large residual velocities relative to the provisional rotation-curve solution. The catalog mentioned above also gives standard errors of individual distance and radial velocities.

We adopted 150 tangent-point radial velocities of H I clouds from Fich *et al.* (1989). Note that published H I and H II radial velocities are traditionally corrected for the solar motion relative to the standard apex assumed to coincide with the local standard of rest (LSR), and we therefore first converted them into heliocentric radial velocities.

METHOD OF ANALYSIS

We used the techniques of maximum-likelihood and statistical parallax (including its simplified version) to compute the kinematic parameters and refine the distance scales involved. See Murray (1986) for a description of the principal ideas of the statistical-parallax method used in this paper. The tangential velocity of a star is computed from its proper motion and distance and therefore depends on the adopted distance scale, whereas radial velocities are distance independent. The essence of the method is to reconcile the fields of radial and tangential velocities in terms of some model of the field of systematic motions and ellipsoidal distribution of residual velocities. A number of authors applied this method with success. Hawley *et al.* (1986); Popovski and Gould (1998), Gould and Popowski (1998), Fernley *et al.* (1998), Popowski (1998), Fernley *et al.* (1998), Tsujimoto *et al.* (1998), and Dambis and Rastorguev (2001) used it to refine the distance scale of RR Lyrae type variables. In our previous paper (Rastorguev *et al.* 1999) we applied this method for the first time, albeit in a somewhat simplified form ignoring the scatter of absolute magnitudes, to analyze the space velocity field of young objects of the Galactic disk, which are characterized by small residual velocity dispersions.

In this paper we also apply a simplified version of the statistical-parallax technique (as used, e.g., by Feast *et al.* 1998), based on reconciling the kinematic parameters inferred separately from radial velocities and proper motions. Thus, it is well known that Oort's constant A inferred from proper motions is much less sensitive to the adopted distance scale than is the value of the same constant inferred from radial velocities. This allows not only the kinematic parameters to be determined but also the distance scale of objects under study to be refined.

Consider now a model of the field of space velocities that includes both differential rotation and effects due to a spiral density wave. The residual velocity of a star can be written in the form of the following column vector:

$$\Delta \mathbf{V} = \mathbf{V}_{\text{obs}} - \mathbf{V}_{\text{sys}} = \mathbf{V}_{\text{obs}} - \mathbf{V}_{\text{sun}} - \mathbf{V}_{\text{rot}} - \mathbf{V}_{\text{spir}},$$

where \mathbf{V}_{obs} is the observed space velocity; \mathbf{V}_{sys} , the total velocity of systematic motions including: \mathbf{V}_{sun} , the mean heliocentric velocity of the sample studied; \mathbf{V}_{rot} , the contribution of Galactic differential rotation; and \mathbf{V}_{spir} , the perturbation due to the spiral density wave. To allow for spiral-pattern effects, we used a very simple kinematic model based on linear density-wave theory by Lin *et al.* (1969) with the perturbation of potential in the form of a running wave:

$$\Phi_S = A_\Phi \cos \chi,$$

where $A_\Phi < 0$ is the amplitude of perturbations and

$$\chi = m(-\theta + \cot i \ln(R/R_0)) + \chi_0,$$

the phase angle of the object in the wave (it increases toward the Galactic center). Here m is the number of arms; θ , the position angle of the object (measured in the direction of rotation); i , the pitch angle of spiral arms ($i < 0$ for trailing spirals); χ_0 , the phase angle of the Sun; and R and R_0 , the Galactocentric distances of the Sun and the object, respectively. The radial V_R (which in the arm is directed toward the Galactic center) and azimuthal V_θ (directed along differential rotation at the outer edge of the arm) components of velocity perturbation can be written in the following form:

$$V_R = f_R \cos \chi, \quad V_\theta = f_\theta \sin \chi,$$

where f_R and f_θ are the amplitudes of velocity perturbations (Rohlf's 1977):

$$f_R = \frac{kA_\Phi}{\kappa} \frac{\nu}{1 - \nu^2} F_\nu^{(1)}(x),$$

$$f_\theta = -\frac{kA_\Phi}{2\Omega} \frac{1}{1 - \nu^2} F_\nu^{(2)}(x).$$

We now use standard designations:

$$k = \frac{m \cot i}{R}, \quad \kappa = 2\Omega \sqrt{1 - \frac{A}{\Omega}},$$

$$x = \left(\frac{k\sigma_u}{\kappa} \right)^2, \quad \nu = \frac{m(\Omega_P - \Omega)}{\kappa}.$$

Here, k is the radial wavenumber; κ , the epicyclic frequency; A , Oort's constant; $F_\nu^{(1)}(x)$ and $F_\nu^{(2)}(x)$, the reduction factors; x , the Toomre instability parameter; σ_u , the dispersion of radial velocities; ν , the relative frequency with which the object rotating in a circular orbit meets a passing spiral wave; Ω , the angular velocity of differential Galactic rotation; and Ω_P , the angular velocity of the rigid rotation of the spiral pattern (i.e., the pattern speed).

Residual space velocities are usually assumed to have a three-dimensional normal distribution:

$$f(\Delta \mathbf{V}) = (2\pi)^{-3/2} |L_{\text{obs}}|^{-1/2} \times \exp \left\{ -0.5 \Delta \mathbf{V}^T \times L_{\text{obs}}^{-1} \times \Delta \mathbf{V} \right\},$$

where L_{obs} is the matrix of covariances. The covariance matrix in our previous paper (Rastorguev *et al.* 1999) included only the ellipsoidal velocity distribution and the errors of radial velocities and proper motions, which is quite a justifiable approach in the case of small errors in the adopted distances. The latter are related to the dispersion of absolute magnitudes as follows:

$$\sigma_M^2 = 4.71 \langle (\delta r/r)^2 \rangle.$$

Here, angular braces mean averaging over the distribution of distance errors. The covariance matrix can be easily shown (Rastorguev 2001) to have the following form:

$$L_{\text{obs}} = L_{\text{loc},e} + L_{\text{err}} + 0.21\sigma_M^2 r_t^2 (P \times L_1 \times P') \\ - 0.21\sigma_M^2 p r_t (M \times L_2 \times P') \\ + 0.21\sigma_M^2 p^2 (M \times L_3 \times M'),$$

where matrices L_1, L_2, L_3, M , and P are equal to

$$L_1 = \frac{d\mathbf{V}_{\text{sys}}}{dr_t} \times \frac{d\mathbf{V}_{\text{sys}}^T}{dr_t}, \quad L_2 = 2\mathbf{V}_{\text{sys}} \times \frac{d\mathbf{V}_{\text{sys}}^T}{dr_t}, \\ L_3 = G_S \times L_{S,0} \times G_S^T + \mathbf{V}_{\text{sys}} \times \mathbf{V}_{\text{sys}}^T,$$

$$M = \begin{pmatrix} 0 & 0 & 0 \\ 0 & 1 & 0 \\ 0 & 0 & 1 \end{pmatrix}, \quad P = \begin{pmatrix} 1 & 0 & 0 \\ 0 & p & 0 \\ 0 & 0 & p \end{pmatrix},$$

respectively, and the formulas for matrices $G_S, L_{\text{loc},e}, L_{\text{err}}$, and $L_{S,0}$ can be found in the paper by Rastorguev *et al.* (1999). Here p is the distance-scale factor defined as:

$$p = r_0/r_t,$$

where r_0 and r_t are the adopted (usually photometric) and true distance, respectively.

We inferred the unknown parameters including the scale factor p using the maximum-likelihood method, i.e., by minimizing the following function with summation taken over all objects of the sample under study:

$$\text{LF} = - \sum_{i=1}^N \ln f(\Delta\mathbf{V}).$$

When refining the distance scale by reconciling the values of Oort's constant A , we set $p = 1$. We computed the parameter errors using the method proposed by Hawley *et al.* (1986).

RESULTS AND DISCUSSION

Kinematics of the Sample of Long-Period Cepheids and OSC

Our main task was twofold: to refine the distance scale of objects considered and to construct the rotation curve of the corresponding subsystem. We first applied the maximum-likelihood method to our sample of Cepheids and OSC with heliocentric distances $r < 4$ kpc and ignored spiral-pattern effects in the velocity field. Because the eventual correlation between the solar Galactocentric distance R_0 and

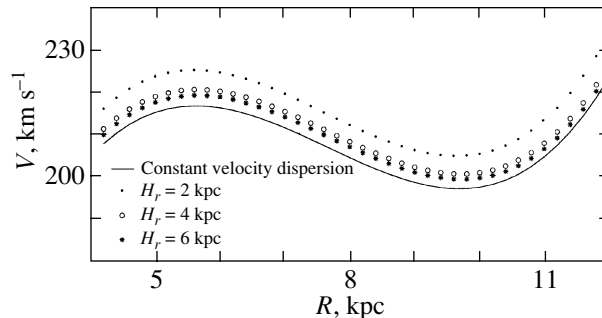


Fig. 1. Galactic rotation curves inferred with different scale lengths H_r and assuming constant velocity dispersion.

the distance- scale factor prevents simultaneous determination of these parameters, and because of the uncertainty in the determination of R_0 , we performed our computations twice with the two most commonly adopted values: $R_0 = 7.5$ and 8.5 kpc. We determined the angular velocity of Galactic rotation Ω_0 from space velocities of Cepheids and OSC and then used it to construct the Galactic rotation curve based on the radial velocities of all objects considered.

How distance errors affect the results. To elucidate the effect of the distance errors on the results obtained, we repeated our computations with three different standard errors of absolute-magnitude calibration: 0^m1 , 0^m15 , and 0^m2 for Cepheids and OSC. We set $R_0 = 7.5$ kpc and $p = 1$ in all three cases. The results are listed in Table 1. The columns of this table give the standard error of the absolute magnitude; heliocentric velocity components of the sample; velocity-ellipsoid axes; and rotation-curve parameters. The inferred kinematic parameters can be seen to be virtually independent of the adopted σ_M , and therefore in the following computations we used a compromise value of $\sigma_M = 0^m15$, which agrees with the scatter of the period-luminosity relation for the Cepheids members of open clusters (Berdnikov *et al.* 1996).

The effect of the variation of velocity dispersion with galactocentric distance. The study of the kinematics and space distribution of objects in the disks of other galaxies showed that the disk surface brightness and velocity dispersion decrease exponentially with galactocentric distance, and the squared velocity dispersion is proportional to the surface density (van den Kruit and Freeman 1986; Bottema 1993). The corresponding scale length for our Galaxy can be estimated only indirectly and is most likely confined between 2 and 6 kpc depending on the age of the subsystem studied (Lewis and Freeman 1989; Kent *et al.* 1991; Malhotra 1995; Dehnen and Binney 1998; Freudenreich 1998; Drimmel and Spergel 2001). Let us assume that radial velocity

Table 1. Kinematic parameters of the Cepheid + OSC sample inferred adopting different standard errors of absolute magnitudes

σ_M	u_0	ν_0	w_0	σ_u	σ_ν	σ_w	$\Omega_0,$ km s ⁻¹ kpc ⁻¹	$\Omega',$ km s ⁻¹ kpc ⁻²	$\Omega'',$ km s ⁻¹ kpc ⁻³
	km s ⁻¹								
0 ^m :10	-6.34	-12.39	-6.95	12.90	8.02	7.21	27.71	-4.66	1.18
0 ^m :15	-6.31	-12.33	-6.96	12.82	7.93	7.19	27.71	-4.66	1.17
0 ^m :20	-6.27	-12.25	-6.98	12.72	7.81	7.15	27.71	-4.65	1.15

Table 2. Kinematic parameters of the Cepheid + OSC sample inferred with different scale lengths of the assumed exponential radial decrease of velocity dispersions

$H_r,$ kpc	$u_0,$	$\nu_0,$	$w_0,$	$\sigma_u,$	$\sigma_\nu,$	$\sigma_w,$	$\Omega_0,$ km s ⁻¹ kpc ⁻¹	$\Omega',$ km s ⁻¹ kpc ⁻²	$\Omega'',$ km s ⁻¹ kpc ⁻³
	km s ⁻¹								
2	-6.77	-12.45	-6.94	14.40	7.88	7.15	28.76	-4.84	1.23
4	-6.35	-12.34	-6.95	13.25	7.93	7.17	28.22	-4.74	1.18
6	-6.30	-12.32	-6.95	13.04	7.94	7.18	28.05	-4.71	1.17

Table 3. Kinematic parameters and the distance-scale factor for the Cepheid + OSC sample inferred via statistical parallaxes

$R_0,$ kpc	p	$u_0,$	$\nu_0,$	$w_0,$	$\sigma_u,$	$\sigma_\nu,$	$\sigma_w,$	$\Omega_0,$ km s ⁻¹ kpc ⁻¹	$\Omega',$ km s ⁻¹ kpc ⁻²	$\Omega'',$ km s ⁻¹ kpc ⁻³
		km s ⁻¹								
7.5	0.86	-7.24	-11.51	-8.06	13.70	8.03	8.55	26.93	-4.27	0.94
8.5	0.84	-7.21	-12.33	-8.24	13.65	8.15	8.76	26.61	-3.66	0.73
Standard errors	±0.05	±2.10	±1.76	±1.61	±1.62	±1.18	±1.68	±1.35	±0.24	±0.19

dispersion varies exponentially with Galactocentric radius:

$$\sigma_u = \sigma_u^0 \exp\left(-\frac{R - R_0}{2H_r}\right),$$

Table 4. The first derivative of angular velocity inferred separately from radial velocities V_r and proper motions μ of the Cepheid + OSC sample and the resulting distance-scale factor

Method	$R_0,$ kpc	$\Omega'(V_r),$ km s ⁻¹ kpc ⁻²	$\Omega'(\mu),$ km s ⁻¹ kpc ⁻²	p
1	7.5	-4.67	-4.53	0.97
2	7.5	-4.68	-4.42	0.94
1	8.5	-4.04	-3.97	0.98
2	8.5	-4.06	-3.88	0.96
Standard errors		±0.26	±0.34	±0.09

where σ_u^0 is the radial velocity dispersion in the solar neighborhood and H_r , the disk scale length parameter. As is evident from our Table 1 (see also results of Rastorguev *et al.* (1999) and Dehnen and Binney (1998)), in the neighborhood of the Sun the components of the velocity dispersion tensors of both the classical Cepheids + OSC and local MS-star sample obey the following Lindblad relation to a good accuracy:

$$\sigma_\nu = \sigma_u \frac{\kappa}{2\Omega}.$$

It is possible, assuming that this relation is obeyed at every point of the disk for the current values of angular rotation velocity and epicyclic frequency, to determine how the inferred kinematic parameters depend on the adopted disk scale length. In this analysis we can neglect the effect of the variation of the vertical velocity dispersion σ_w with Galactocentric distance, because, first, it is insignificant compared to the errors of tangential velocities V_b , and, second,

the allowance for the dependence of vertical velocity dispersion on Galactocentric distance has virtually no effect on the results obtained. Table 2 presents the kinematic parameters computed with $R_0 = 7.5$ kpc, and $p = 1$. The tabulated velocity-ellipsoid axes refer to the solar neighborhood. Note that Ω_0 is sensitive to the adopted scale length parameter.

Figure 1 shows how the inferred rotation curve changes with the adopted scale length. Although the exact scale for our sample is unknown, an analysis of the results of Kent *et al.* (1991) leads us to conclude that young subsystems are characterized by a relatively shallower decrease of radial dispersion with Galactocentric distance. According to our results, the rotation curve for $H_r = 2$ kpc is 9 km s^{-1} higher than if computed for constant velocity dispersion. Dehnen and Binney (1998) inferred a scale length of $\sim 2\text{--}2.5$ kpc for old main-sequence stars; Drimmel and Spergel (2001) found a scale length of $0.28R_0$ by analyzing COBE/DIRBE data (note that both old and young stars contribute to infrared radiation). Since no accurate data are available about the relation between surface brightness and velocity dispersion, hereafter we assume that velocity dispersion remains constant along Galactocentric radius.

Refining the distance scale. Table 3 lists the kinematic parameters inferred treating the distance-scale factor as an unknown parameter. The initial distances to Cepheids and OSC are on the short distance scale. As is evident from the table, the distance-scale factor depends only slightly on the adopted R_0 . Judging by these results, the adopted distance scale should be increased by 14–16%.

Besides the rigorous method of statistical parallaxes, we also used its simplified version, which involves comparing the values of the first derivative of angular velocity Ω' inferred separately from radial velocities with proper motions. We determined the kinematic and rotation-curve parameters of the sample under study from independent maximum-likelihood solutions based on radial velocities and proper motions. It can be easily seen that radial velocities of stars of flat subsystems allow neither w_0 nor σ_w to be accurately constrained. We therefore inferred Ω' in two ways: (1) by computing the heliocentric space velocity components u_0, ν_0, w_0 and vertical velocity dispersion σ_w of the sample under study from space velocities, and then fixing these values in separate radial velocity and proper-motion solutions; and (2) by substituting u_0 and ν_0 inferred from radial velocities into the proper-motion solution and substituting w_0 and σ_w inferred from proper motions into the radial velocity solution. Table 4 lists the resulting Ω' and distance-scale factors $p = \Omega'(\mu)/\Omega'(V_r)$.

The resulting mean distance-scale factor for the Cepheid+OSC subsystem is equal to $p = 0.96$ for $R_0 = 7.5$ kpc (with $\Omega' = -4.50 \text{ km s}^{-1} \text{ kpc}^{-2}$) and $p = 0.97$ for $R_0 = 8.5$ kpc (with $\Omega' = -3.95 \text{ km s}^{-1} \text{ kpc}^{-2}$). Again, we note a weak dependence of the distance-scale factor on the adopted solar Galactocentric distance (see Table 5).

Noteworthy are (see Tables 3 and 5) systematic differences between the distance-scale factors given by the statistical-parallax technique (~ 0.86) and by its simplified modification (~ 0.96). We analyzed the problem for possible biases using numerical simulations. To this end, we used the real coordinates and initial distances to the objects of our sample and simulated their “true” space velocities based on the earlier determined values of kinematic and rotation-curve parameters. We then added normally distributed errors to the “true” distances and space velocities and redetermined the kinematic parameters and distance-scale factor using both the rigorous statistical-parallax technique (space velocities) and its simplified modification. We set velocity errors based on the typical errors of observational data and ellipsoidal distribution of residual velocities. One hundred numerical simulations yielded a mean distance-scale factor of $p = 1.00 \pm 0.05$ and $p = 1.01 \pm 0.07$ by making inferences from space velocities or by comparing the first derivatives of angular velocity, respectively. The possible distance-scale factors were confined to the (0.85–1.15) interval, with, on the average, correlated deviations of the two values from unity. We cannot unambiguously choose between the two approaches to the distance-scale refinement. Since it is logical to associate the short and long distance scales with $R_0 = 7.5$ kpc and $R_0 = 8.5$ kpc, respectively, hereafter we inferred the kinematic parameters assuming that the Cepheid+OSC distance-scale factors of $p = 0.96$ and 0.84 correspond to $R_0 = 7.5$ and 8.5 kpc, respectively. In support of this conclusion, we determined R_0 from space velocities with fixed p . Our analysis yielded $R_0 = (7.4 \pm 1.0)$ and (8.3 ± 1.0) kpc for $p = 0.96$ and 0.84, respectively. The large errors of the resulting R_0 are due to the small size of the data sample used.

Determination of Ω_0 from radial velocities using Lindblad’s relation. Note that the fact that the velocity dispersions of Cepheids and OSC obey the Lindblad relation allows the angular velocity of rotation Ω_0 at the solar Galactocentric distance to be estimated independently from radial velocities exclusively. When computing the kinematic parameters, the idea is to set as unknown only the radial velocity dispersion σ_u^0 at the solar Galactocentric distance and to determine the ratio of velocity ellipsoid axes from the Lindblad relation while setting the angular velocity and its derivative equal to their local values for each

Table 5. Kinematic parameters of the Cepheid + OSC sample inferred from space velocities using the mean distance-scale factors (determined by comparing the first derivatives of angular velocity)

R_0 , kpc	u_0	ν_0	w_0	σ_u	σ_ν	σ_w	Ω_0 , km s ⁻¹ kpc ⁻¹	Ω' , km s ⁻¹ kpc ⁻²	Ω'' , km s ⁻¹ kpc ⁻³
	km s ⁻¹								
7.5	-6.55	-12.11	-7.25	13.04	7.92	7.55	27.47	-4.54	1.09
8.5	-6.38	-12.98	-7.18	12.80	8.04	7.44	27.37	-3.99	0.90
Standard errors	±1.77	±1.71	±1.24	±1.49	±1.10	±1.22	±1.39	±0.24	±0.19

Table 6. Kinematic parameters of the blue-supergiant sample

R_0 , kpc	u_0	ν_0	w_0	σ_u	σ_ν	σ_w	Ω_0 , km s ⁻¹ kpc ⁻¹	Ω' , km s ⁻¹ kpc ⁻²	Ω'' , km s ⁻¹ kpc ⁻³
	km s ⁻¹								
7.5	-6.04	-10.92	-7.12	11.49	8.96	5.13	29.60	-4.76	0.89
8.5	-6.18	-11.33	-7.86	11.63	9.41	5.71	29.14	-4.00	0.60
Standard errors	±1.93	±1.73	±1.08	±1.42	±1.14	±1.03	±1.62	±0.32	±0.53

Table 7. Kinematic and rotation-curve parameters inferred from H II data

R_0 , kpc	u_0	ν_0	σ_u	σ_ν	Ω' , km s ⁻¹ kpc ⁻²	Ω'' , km s ⁻¹ kpc ⁻³
	km s ⁻¹					
7.5	-8.11	-14.88	6.70	6.91	-4.77	1.26
8.5	-7.92	-15.73	6.56	7.03	-4.08	1.01
Standard errors	±1.71	±1.19	±2.07	±1.14	±0.27	±0.22

object. The resulting likelihood function therefore depends explicitly on the unknown angular velocity Ω_0 . We applied this method with fixed $w_0 = -7$ km s⁻¹ and $\sigma_w = 7$ km s⁻¹ to the radial velocities of Cepheids and OSC with $p = 0.96$ and $R_0 = 7.5$ kpc to obtain $\Omega_0 = (26.5 \pm 8.7)$ km s⁻¹ kpc⁻¹. The large error of the inferred angular velocity is fully explained by the errors of the inferred velocity dispersions, which are equal to 1.2–1.7 km s⁻¹ (see Table 5). The surprisingly good agreement between the angular velocity values inferred from space and radial velocities indicates that the Lindblad relation is obeyed accurately enough throughout the entire space region studied.

Kinematics of the Blue-Supergiant Sample

We applied the maximum-likelihood technique to a sample of 102 blue supergiants. The dispersion of the inferred absolute magnitudes for these stars is higher than for Cepheids and OSC and is equal to $\sigma_M \approx 0^m.38$ (Dambis 1990). We estimated the distance-scale factor using the two methods

described above. The maximum-likelihood method applied to space velocities of stars yielded $p = 0.97 \pm 0.08$, whereas a comparison of the first derivatives of angular velocity determined separately from radial velocities and proper motions yielded $p = 1.09 \pm 0.16$ (error estimated approximately). Both results agree fairly well with the correction factor to the blue-supergiant distance scale ($p = 1.03 \pm 0.04$) inferred from practically the same sample by comparing photometric and HIPPARCOS trigonometric parallaxes (Dambis *et al.* 2001). As in the case of the Cepheid and OSC sample, the distance-scale correction factors given by the two methods differ systematically by ~ 0.1 . Table 6 lists the final kinematic parameters for the blue-supergiant sample.

Blue supergiants yielded somewhat higher angular velocity Ω_0 compared to what we inferred from the Cepheid and OSC sample, but the difference is within the quoted errors. The systematic difference between the two angular velocity values is partly due to the specifics of the space distribution of objects involved. The most reliable estimates of angular velocity are those inferred from objects lying in the vicinity of the

Table 8. Galactic rotation curve $V(R)$ for the short and long distance scales

R , kpc	$V(R)$, km s ⁻¹ $R_0 = 7.5$ kpc	$V(R)$, km s ⁻¹ $R_0 = 8.5$ kpc	R , kpc	$V(R)$, km s ⁻¹ $R_0 = 7.5$ kpc	$V(R)$, km s ⁻¹ $R_0 = 8.5$ kpc
2.0	198.1	198.2	8.2	201.6	227.5
2.1	199.9	201.3	8.3	200.7	227.0
2.3	201.3	203.8	8.4	199.8	226.4
2.4	202.4	205.9	8.6	199.0	225.8
2.6	203.3	207.6	8.7	198.3	225.2
2.7	204.0	209.0	8.9	197.6	224.6
2.8	204.6	210.3	9.0	196.9	224.0
3.0	205.2	211.4	9.1	196.3	223.3
3.1	205.7	212.3	9.3	195.8	222.7
3.3	206.2	213.2	9.4	195.4	222.1
3.4	206.7	213.9	9.6	195.1	221.5
3.5	207.2	214.7	9.7	194.8	220.9
3.7	207.8	215.4	9.8	194.6	220.4
3.8	208.3	216.2	10.0	194.5	219.9
4.0	208.9	216.9	10.1	194.5	219.4
4.1	209.5	217.6	10.3	194.6	219.0
4.2	210.1	218.4	10.4	194.8	218.7
4.4	210.6	219.1	10.5	195.0	218.5
4.5	211.2	219.9	10.7	195.4	218.3
4.7	211.7	220.7	10.8	195.8	218.2
4.8	212.2	221.5	11.0	196.3	218.1
4.9	212.6	222.3	11.1	196.9	218.2
5.1	212.9	223.1	11.2	197.6	218.3
5.2	213.2	223.8	11.4	198.4	218.5
5.4	213.4	224.6	11.5	199.2	218.9
5.5	213.5	225.3	11.7	200.2	219.3
5.6	213.5	226.0	11.8	201.2	219.8
5.8	213.4	226.6	11.9	202.4	220.4
5.9	213.3	227.2	12.1	203.6	221.1
6.1	213.0	227.7	12.2	205.0	221.9
6.2	212.7	228.2	12.4	206.4	222.8
6.3	212.2	228.6	12.5	208.0	223.7
6.5	211.7	229.0	12.6	209.8	224.8
6.6	211.1	229.2	12.8	211.6	226.0
6.8	210.5	229.4	12.9	213.7	227.2
6.9	209.7	229.5	13.1	215.9	228.5
7.0	208.9	229.6	13.2	218.3	229.9
7.2	208.1	229.6	13.3	220.9	231.4
7.3	207.2	229.5	13.5	223.7	233.0
7.5	206.3	229.3	13.6	226.7	234.6
7.6	205.4	229.0	13.8	230.0	236.3
7.7	204.4	228.8	13.9	233.6	238.0
7.9	203.5	228.4	14.0	237.4	239.8
8.0	202.5	228.0			

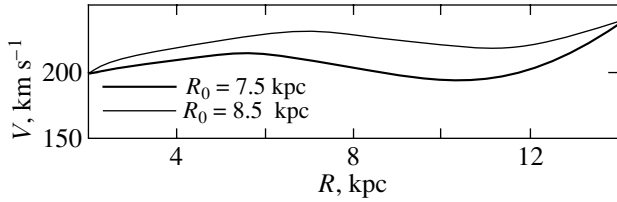


Fig. 2. Galactic rotation curve $V(R)$ for the short ($R_0 = 7.5$ kpc) and long ($R_0 = 8.5$ kpc) distance scales.

“tangent circle” (it is the circle in the Galactic plane with the interval connecting the Sun and the Galactic center as its diameter), because, in the corresponding conditional proper-motion equations, the coefficients at the angular-velocity derivatives are close to zero (Glushkova *et al.* 1999). The proper motions of 23 blue supergiants lying in the vicinity of the “tangent circle” yielded $\Omega_0 = (27.91 \pm 2.79)$ km s⁻¹ kpc⁻¹; i.e., the angular velocities inferred from two samples agree well with each other. This result justifies the subsequent use of blue supergiants for constructing the combined rotation curve over a wide interval of Galactocentric distances.

Kinematics of Ionized Hydrogen

The only way to match the distance scales of H II and stars is to compare the first derivatives of angular velocity inferred from line-of-sight and space velocities for gas and stars, respectively. Given that the scatter of velocities along the z -coordinate has virtually no effect on the radial velocities of the thin-disk objects, we fixed $w_0 = -7$ km/s and $\sigma_w = \sigma_v$. Table 7 lists the kinematic and rotation-curve parameters inferred from H II data for $r < 4$ kpc. In this interval of Galactocentric distances the first derivatives of angular velocity for gas (inferred from radial velocities) and stars (inferred from space velocities) are estimated at either -4.77 and -4.54 km s⁻¹ kpc⁻², respectively (if $R_0 = 7.5$ kpc) implying the H II distance-scale correction factor $p = 0.95$, or -4.08 and -3.66 km s⁻¹ kpc⁻², respectively (if $R_0 = 8.5$ kpc) implying the H II distance-scale correction factor $p = 0.90$. Note that, as expected, the velocity ellipsoid axes inferred for gas do not obey the Lindblad relation, but $\sigma_u \approx \sigma_v$.

Constructing the Rotation Curve

The good agreement between the mean heliocentric velocity components of different young-object samples allows us to construct the rotation curve over a sufficiently wide interval of Galactocentric distances, 2–14 kpc, using radial velocities of both stars and gas. Figure 2 shows the rotation curves

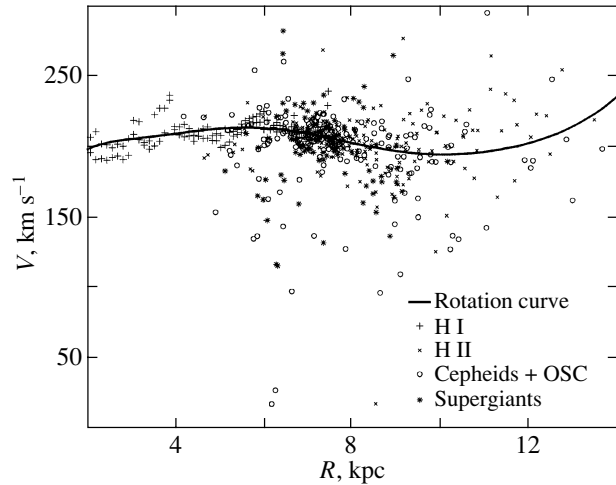


Fig. 3. Galactic rotation curve $V(R)$ for the short distance scale ($R_0 = 7.5$ kpc) with young-object data points superimposed.

$V(R)$ inferred from the entire sample of young objects (OSC + Cepheids + supergiants + H I + H II) for $R_0 = 7.5$ and 8.5 kpc. These rotation curves are tabulated in Table 8. Here we expanded the difference of angular velocities into a seventh-order Taylor series in the vicinity of R_0 , and computed the velocity ellipsoid axes separately for neutral and ionized hydrogen, blue supergiants, and for Cepheids + OSC (see Table 9) with the distances to all objects matched to each other. The resulting local centroid velocity and Oort’s constant A are equal to $V(R_0) = (206 \pm 10)$ km s⁻¹, $A = (17.1 \pm 0.5)$ km s⁻¹ kpc⁻¹ and $V(R_0) = (226 \pm 12)$ km s⁻¹, $A = (15.4 \pm 0.6)$ km s⁻¹ kpc⁻¹ for the short and long distance scale, respectively.

Figure 3 shows the rotation curve for the short distance scale ($R_0 = 7.5$ kpc) with the data points for individual objects computed using the following formula:

$$V = R\Omega_0 + \frac{R}{R_0 \sin l \cos b} (V_r - V_{\text{sun},r}),$$

where $V_{\text{sun},r}$ is the radial projection of the heliocentric velocity of the sample considered. As is evident from the figure, the scatter of V about the rotation curve is due mainly to small $\sin l$. Note that systematic differences between HI velocities may be manifestations of a barlike structure at the center of the Galaxy (Freudenreich 1998). The gas-stellar disk of the Galaxy is well known to show appreciable warp in the direction $l \approx 90^\circ$ at Galactocentric distances > 10 kpc. Our rotation curve therefore applies only to the part of the Galactic disk where warp is insignificant.

Table 9. Heliocentric velocity components and velocity-ellipsoid axes for the young-object sample

Objects	σ_u ,	σ_ν ,	σ_w^* ,	u_0	ν_0	w_0^*
	km s ⁻¹					
Cepheids + OSC	13.30	7.59	7.55	-9.17	-12.98	-7.25
Standard errors	±1.79	±0.41	—	»	»	»
Supergiants	14.17	10.00	5.13	»	»	»
Standard errors	±0.51	±2.12	—	»	»	»
H II	6.71	7.19	5.0	»	»	»
Standard errors	±0.60	±0.93	—	»	»	»
H I	6.60	6.05	5.0	»	»	»
Standard errors	—	±0.34	—	±0.48	±0.78	—

* Parameters fixed at values inferred from the space-velocity solution.

Table 10. Parameters of the spiral pattern ($R_0 = 7.5$ kpc)

Objects	m	f_R	f_θ	i	χ_0
		km s ⁻¹		deg	
Cepheids	2	-6.66	-1.40	-6.02	-85.19
OSC	4	-5.51	-0.16	-12.18	-88.05
Standard errors		±2.34	±1.56	±0.72	±14.50
OB-stars	2	-6.64	0.42	-6.55	-97.28
Standard errors		±2.51	±2.31	±0.86	±18.30

Allowing for Spiral-Arm Effects

Our computations showed that young-object samples lag behind the Sun on the average by 13 km s⁻¹. Dehnen and Binney (1998) used HIPPARCOS proper motions and parallaxes of nearby MS stars to find out that the Sun moves ahead of the LSR by 5.25 km s⁻¹. It follows from this that young subsystems lag behind the LSR by ~ 8 km s⁻¹, whereas their velocity dispersion should imply a velocity lag of ≤ 1.5 km s⁻¹. This discrepancy may be due, among other things, to streaming motions induced by spiral arms.

To allow for the spiral-arm effects in the velocity field, we performed our computations in terms of two- and four-armed models of the spiral pattern (see Table 10).

The phase of the Sun with respect to the spiral wave, which is close to $-\pi/2$, indicates that the Sun is situated at the outer edge of the arm; $V_\theta \approx 1.4$ km s⁻¹ (for the Cepheid + OSC sample). We therefore face a discrepancy between the magnitude and direction of the tangential disturbance as inferred from the centroid velocity lag behind the LSR ($V_\theta \approx$

-6.5 km s⁻¹) and the value of the same quantity computed directly in terms of a model of spiral-pattern effects in the velocity field. The discrepancy is beyond the quoted errors. The velocity lag of the centroid of young objects relative to the LSR can be explained by, among other things, noncircular motions of the LSR discussed by a number of authors (Schuter 1982; Clemens 1985) based on their analyses of H I radial velocities. Thus Clemens (1985) inferred an LSR tangential velocity of ~ 7 km s⁻¹ from an analysis of H I motions in the local solar neighborhood. However, Dehnen and Binney (1998) showed that, despite their different ages and velocity dispersions, all main-sequence stars (except late-type B-stars) closely follow a unified theoretical dependence of the sample tangential velocity on velocity dispersion. Streaming motions should be “washed out” by ever increasing velocity dispersion, and we therefore consider the above determinations of the solar velocity relative to the LSR to be quite correct, and thus the discrepancy in question is left unexplained. Interestingly, the heliocentric velocity of B-type stars inferred by Dehnen and Binney agrees well with the velocities we inferred for the young-object samples.

ACKNOWLEDGMENTS

We are grateful to A.M. Mel'nik, E.V. Glushkova, and V.G. Surdin for their assistance and valuable discussions. The work was supported by the Russian Foundation for Basic Research, grant nos. 01-02-06012, 00-02-17804, 99-02-17842, and 01-02-16086; Astronomy State Research and Technology Program; and the Council for the Support of Leading Scientific Schools, grant no. 00-15-96627.

REFERENCES

1. M. Barbier-Brossat and P. Figon, *Astron. Astrophys.*, Suppl. Ser. **142**, 217 (2000).
2. H. Baumgardt, C. Dettbarn, and R. Wielen, *Astron. Astrophys.*, Suppl. Ser. **146**, 251 (2000).
3. L. N. Berdnikov, O. V. Vozyakova, and A. K. Dambis, *Pis'ma Astron. Zh.* **22**, 936 (1996) [*Astron. Lett.* **22**, 838 (1996)].
4. R. Bottema, *Astron. Astrophys.* **275**, 16 (1993).
5. J. Brand and L. Blitz, *Astron. Astrophys.* **275**, 67 (1993).
6. D. P. Clemens, *Astrophys. J.* **295**, 422 (1985).
7. A. K. Dambis, *Pis'ma Astron. Zh.* **16**, 522 (1990) [*Sov. Astron. Lett.* **16**, 224 (1990)].
8. A. K. Dambis, *Pis'ma Astron. Zh.* **25**, 10 (1999) [*Astron. Lett.* **25**, 7 (1999)].
9. A. K. Dambis and A. S. Rastorguev, *Pis'ma Astron. Zh.* **27**, 132 (2001) [*Astron. Lett.* **27**, 108 (2001)].
10. A. K. Dambis, A. M. Mel'nik, and A. S. Rastorguev, *Pis'ma Astron. Zh.* **21**, 331 (1995) [*Astron. Lett.* **21**, 291 (1995)].
11. A. K. Dambis, A. M. Mel'nik, and A. S. Rastorguev, *Pis'ma Astron. Zh.* **27**, 68 (2001) [*Astron. Lett.* **27**, 58 (2001)].
12. A. K. Dambis, E. V. Glushkova, A. M. Mel'nik, and A. S. Rastorguev, *Astron. Astrophys. Trans.* **20**, 161 (2001).
13. W. Dehnen and J. J. Binney, *Mon. Not. R. Astron. Soc.* **298**, 387 (1998).
14. R. Drimmel and D. N. Spergel, *Astrophys. J.* **556**, 181 (2001).
15. M. Duflot, P. Figon, and N. Meyssonier, *Astron. Astrophys.*, Suppl. Ser. **114**, 269 (1995).
16. Yu. N. Efremov, *Sites of Star Formation in Galaxies: Star Complexes and Spiral Arms* (Nauka, Moscow, 1989).
17. M. Feast, F. Pont, and P. Whitelock, *Mon. Not. R. Astron. Soc.* **298**, L43 (1998).
18. J. Fernley, T. G. Barnes, I. Skillen, *et al.*, *Astron. Astrophys.* **330**, 515 (1998).
19. M. Fich, L. Blitz, and A. A. Stark, *Astrophys. J.* **342**, 272 (1989).
20. H. T. Freudenreich, *Astrophys. J.* **492**, 495 (1998).
21. E. V. Glushkova, A. K. Dambis, A. M. Mel'nik, and A. S. Rastorguev, *Astron. Astrophys.* **329**, 514 (1998).
22. E. V. Glushkova, A. K. Dambis, and A. S. Rastorguev, *Astron. Astrophys. Trans.* **18**, 349 (1999).
23. A. Gould and P. Popowski, *Astrophys. J.* **508**, 844 (1998).
24. S. L. Hawley, W. H. Jeffreys, T. G. Barnes III, and Lai Wan, *Astrophys. J.* **302**, 626 (1986).
25. M. Honma and Y. Sofue, *Publ. Astron. Soc. Jpn.* **49**, 453 (1997).
26. D. K. Karimova and E. D. Pavlovskaya, *Astron. Zh.* **50**, 737 (1973) [*Sov. Astron.* **17**, 470 (1973)].
27. S. Kent, T. M. Dame, and J. Fazio, *Astrophys. J.* **378**, 131 (1991).
28. P. N. Kholopov, *Astron. Zh.* **57**, 12 (1980) [*Sov. Astron.* **24**, 7 (1980)].
29. J. R. D. Lepine, Yu. N. Mishurov, and S. Yu. Dedikov, *Astrophys. J.* **546**, 234 (2001).
30. J. R. Lewis and K. C. Freeman, *Astron. J.* **97**, 139 (1989).
31. C. C. Lin, C. Yuan, and F. H. Shu, *Astrophys. J.* **155**, 721 (1969).
32. S. Malhotra, *Astrophys. J.* **448**, 138 (1995).
33. F. Maeder and G. Meynet, *Astron. Astrophys.*, Suppl. Ser. **89**, 451 (1991).
34. A. M. Mel'nik, A. K. Dambis, and A. S. Rastorguev, *Pis'ma Astron. Zh.* **27**, 611 (2001) [*Astron. Lett.* **27**, 521 (2001)].
35. M. R. Merrifield, *Astron. J.* **103**, 1552 (1992).
36. Yu. N. Mishurov, E. D. Pavlovskaya, and A. A. Suchkov, *Astron. Zh.* **56**, 268 (1979) [*Sov. Astron.* **23**, 147 (1979)].
37. Yu. N. Mishurov, I. A. Zenina, A. K. Dambis, *et al.*, *Astron. Astrophys.* **323**, 775 (1997).
38. C. A. Murray, *Vectorial Astrometry* (A. Hilger, Bristol, 1983; Naukova Dumka, Kiev, 1986).
39. I. I. Nikiforov, *Astron. Zh.* **76**, 403 (1999) [*Astron. Rep.* **43**, 345 (1999)].
40. I. I. Nikiforov and I. V. Petrovskaya, *Astron. Zh.* **71**, 725 (1994) [*Astron. Rep.* **38**, 642 (1994)].
41. F. Pont, M. Mayor, and G. Burki, *Astron. Astrophys.* **285**, 415 (1994).
42. P. Popowski and A. Gould, *Astrophys. J.* **506**, 259 (1998).
43. A. S. Rastorguev, Determination of Rotation Curve and Scale of Distance in Galaxy, <http://www.astronet.ru:8101/db/msg/1172553>.
44. A. S. Rastorguev, E. V. Glushkova, A. K. Dambis, and M. V. Zabolotskikh, *Pis'ma Astron. Zh.* **25**, 689 (1999) [*Astron. Lett.* **25**, 595 (1999)].
45. A. S. Rastorguev, E. V. Glushkova, M. V. Zabolotskikh, and H. Baumgardt, *Astron. Astrophys. Trans.* **20**, 103 (2001).
46. K. Rohlfs, *Lectures on Density Wave Theory* (Springer-Verlag, Berlin, 1977; Mir, Moscow, 1980).
47. W. L. H. Shuter, *Mon. Not. R. Astron. Soc.* **199**, 109 (1982).
48. J. Torra, D. Fernandez, F. Figueras, and F. Comeron, *Astrophys. Space Sci.* **272**, 109 (2000).
49. T. Tsujimoto, M. Miyamoto, and Y. Yoshii, *Astrophys. J. Lett.* **492**, L79 (1998).
50. P. C. van der Kruit and K. C. Freeman, *Astrophys. J.* **303**, 556 (1986).

Translated by A. Dambis